Psychiatry Research: Neuroimaging 324 (2022) 111492

Contents lists available at ScienceDirect

Psychiatry Research: Neuroimaging

journal homepage: www.elsevier.com/locate/psychresns

Variability and concordance of sulcal patterns in the orbitofrontal cortex: A twin study

Vanessa Troiani *, Will Snyder, Shane Kozick, Marisa A Patti, Donielle Beiler

Geisinger Autism and Developmental Medicine Institute, 120 Hamm Drive, Suite 2A, Lewisburg, PA 17837, United States

ARTICLE INFO

Keywords:
Sulcogyral
Morphometry
Prefrontal cortex
Magnetic resonance imaging
Heritability
Neurogenetics

ABSTRACT

Sulcogyral patterns have been identified in the orbitofrontal cortex (OFC) based on the continuity of the medial and lateral orbital sulci. Pattern types are named according to their frequency in the population, with Type I present in ~60%, Type II in ~25%, Type III in ~10%, and Type IV in ~5%. Previous work has demonstrated that psychiatric conditions with high estimated heritability (e.g. schizophrenia, bipolar disorder) are associated with reduced frequency of Type I patterns, but the general heritability of the OFC sulcogyral patterns is unknown. We examined concordance of OFC patterns in 304 monozygotic (MZ) twins relative to 172 dizygotic (DZ) twins using structural magnetic resonance imaging data. We find that the frequency of pattern types within MZ and DZ twins are similar and bilateral concordance rates across all pattern types in DZ twins were 14% and 21% for MZ twins. Results from follow-up analyses confirm that continuity in the rostral-caudal direction is an important source of variability within the OFC, and subtype analyses indicate that variability is present in other sulci that are not represented by overall OFC pattern type. Overall, these results suggest that OFC sulcogyral patterns may reflect important variance that is not genetic in origin.

1. Introduction

The brain's surface is made up of sulci (grooves) and gyri (ridges) that together create the distinct folded (sulcogyral) appearance of the brain. The orbitofrontal cortex (OFC) is one brain region with a great deal of individual differences in sulcogyral variability. For example, the sulcal group formed by the intersection of the medial, lateral, and transverse sulci within the OFC has been proposed as a potential morphological marker for various psychiatric disorders, including schizophrenia (Chakirova et al., 2010; Isomura et al., 2017; Lavoie et al., 2014; Nakamura et al., 2007; Takayanagi et al., 2010) and bipolar disorder (Patti and Troiani, 2018). This sulcal group is commonly referred to as the "H-sulcus" and four pattern types have been identified in individuals (Type I, II, III, IV), based on the continuity of the medial orbital sulcus (MOS) and lateral orbital sulcus (LOS) (Chiavaras and Petrides, 2000). These pattern types are named according to frequency in the general population, with Type 1 identified in ~60%, Type 2 in ~25%, Type 3 in ~10%, and Type 4 in ~5% across studies.

Most studies examining OFC sulcogyral patterns have compared frequency of pattern types in patients with schizophrenia to those without psychiatric diagnoses. These studies consistently demonstrate that patients with schizophrenia show decreased prevalence of Type I patterns and increased prevalence of the less common Type II, III, and/or IV patterns (Chakirova et al., 2010; Isomura et al., 2017; Lavoie et al., 2014; Nakamura et al., 2007; Takayanagi et al., 2010). We have also found that patients with bipolar disorder show reduced prevalence of Type I patterns relative to individuals without psychiatric diagnoses (Patti and Troiani, 2018). Additional work has identified atypical frequency in patients with gambling disorder (Li et al., 2019), but no differences in overall pattern frequency differences in obsessive compulsive disorder (Delahoy et al., 2019), cannabis use disorder (Chye et al., 2017), or cocaine use disorder (Patti et al., 2020). Previous findings thus suggest that atypical OFC patterns are not necessarily a general marker that confers risk for all psychiatric disorders, but potentially a transdiagnostic trait dimension that is shared by a few related disorders.

To date, there has not been a study specifically exploring heritability of the OFC H-sulcus in twins. One small candidate gene study examined the role of a single nucleotide polymorphism (SNP) and OFC H-sulcus pattern types in patients with schizophrenia and controls. Although there was no difference in allele frequencies between patients with schizophrenia and controls, the expression of a *Neuroregulin 1* (NRG1)

* Corresponding author.
E-mail address: vtroiani@geisinger.edu (V. Troiani).

https://doi.org/10.1016/j.pscychresns.2022.111492
Received 22 November 2021; Received in revised form 15 March 2022; Accepted 13 May 2022
Available online 14 May 2022

SNP, *SNP8NRG243177*, was associated with Type II expression in SZ patients (Yoshimi et al., 2016). This finding suggests that exploring the genetics of OFC sulcogyral patterns may reveal new insights into factors contributing to OFC pattern differences observed in some individuals with psychiatric disorders. It is thought that individual sulcal morphology within the OFC develops *in utero* and remains stable throughout life (Armstrong et al., 1995), although changes in the OFC H-sulcus throughout development have never been explicitly studied. The human brain is predominantly assembled during the first 6 months of the fetal phase by strong genetic influence (Vasung et al., 2019). During this time, brain development of larger primary sulci occurs with a predictable functional architecture, while smaller, secondary sulci develop later (and more randomly) in the developmental process (Jiang et al., 2021; Garcia et al., 2018). Work in other sulcogyral patterns in the brain has demonstrated consistency in major sulci over the course of adolescent development, despite changes in other brain metrics that occur during this period (Cachia et al., 2016; Tissier et al., 2018). Our knowledge of cortical surface development comes from magnetic resonance images (MRI) of post mortem and in vivo fetal development and has demonstrated that primary cortical folds emerge at 20 weeks gestation, secondary folds follow at 32 weeks and tertiary folds at around term (Habas et al., 2012; Chi et al., 1977, Rajagopalan et al., 2011; Dubois et al., 2008; Dubois et al., 2019). Also see Cachia et al. (2021) for more complete review.

Monozygotic (MZ) twins are the same sex and share nearly 100% of the same genetic information. Dizygotic (DZ) twins can be the same or opposite sex and share approximately 50% of the same genes, like non-twin siblings, though sharing the same environmental exposure profile (*in utero* and developmental) relative to MZ twins. Twin studies can be useful for examining the role of genes in traits, because if MZ twins show more similarity relative to DZ twins, this can be taken as evidence that the trait is strongly influenced by genetic factors. Although the OFC H-sulcus has not been the focus of a genetic study using twins in prior work, several studies have examined the heritability of other brain morphological metrics in a twin study design. While the focus of the current paper is on a more qualitative characterization of OFC H-sulcal patterns, a more common way to extract information about sulci from MRI volumes is to measure various structural features, including cortical thickness, local gyrification, and sulcal depth via automated methods (Lyu et al., 2018). One of the earliest morphometric studies of 19 twin pairs used a correlation analysis to determine the similarity of brain-wide gyral patterns from MRI data and found that while gyral patterns were more visually similar in MZ than in DZ twins, most of the variance appeared to be determined by environmental factors. In the same study, cerebral size was found to be almost entirely determined by genetic factors (Bartley, 1997). Hasan et al. (Hasan et al., 2011) examined the genetic influence on gyrification by comparing the gyrification index (GI; ratio of the total inner contour to outdoor contour of the brain enclosing the cortex) in MZ and DZ twins. MZ and DZ twins showed equivalent similarity based on GI and/or brain volume, again suggesting a combination of genetic and environmental influences on the development of cortical folding and brain volume (Hasan et al., 2011). One other study in twins examined the genetic contribution of surface morphology by measuring an index of gyral and sulcal curvature, surface area, and cortical depth (White, 2002). Their results indicated that the regional gray and white matter volumes were more highly correlated in MZ twin pairs. However, the surface measures showed less correlation among MZ twin pairs compared to DZ twin pairs, also suggesting that these sulcogyral measures are more influenced by environmental factors (White, 2002). Additional studies have found that sulcal patterns measured using sulcal graph matching were more similar in MZ twins (Im et al., 2011) and that some genetic relationships with cortical thickness depend on the age of maturation (Lenroot et al., 2009). For an overview of genetic influences on human brain studies in twins, see review by Peper and colleagues (Peper et al., 2007).

All previous studies of sulcogyral metrics in twin brain imaging studies have relied on quantitative estimates of cortical folding. The more qualitative features of cortex sulcation, such as the sulcogyral pattern within the "H" sulcus, are relatively understudied, but show great potential as a distinct representation of cortical morphology that can be used as a predictive marker of disease (for review, see Cachia et al., 2021). The overarching pattern type of each brain hemisphere can be characterized using a widely established manual characterization procedure. In addition to the overall pattern type of each hemisphere, we have recently published on the importance of characterizing pattern subtypes. Subtypes within each overarching pattern type exist, as there are distinct properties and qualitative variability of other OFC sulci that are not included in the characterization process of the four overarching patterns. Chiavaras & Petrides (Chiavaras and Petrides, 2000) first documented 18 subtypes (6 each in the Type I, II, and III patterns described in the seminal OFC pattern typing paper). Although subtypes are not important or necessary for overall pattern type characterization, they may be important in future work. For example, we have previously demonstrated that patients with cocaine use disorder did not differ in their overall pattern type in the OFC, but showed wider variability in their OFC pattern subtypes (Patti et al., 2020). From this perspective, sulcogyral subtypes as we describe in the current work may be an important measurable factor that contributes to neuroanatomical variance within populations with psychiatric disease.

To our knowledge, no previous work has examined the more qualitative structure of the sulci within the OFC, frequently referred to as the OFC "H" sulcus, in a population of MZ and DZ twins. Here, we use the widely established manual procedure to characterize sulcogyral patterns in the OFC of MZ and DZ twins, in order to evaluate whether there is a genetic contribution to the shape of the H-sulcus. In addition to establishing concordance of overall pattern types within MZ and DZ twin pairs, we also characterize OFC sulcogyral variability using manifold learning and characterization of H-sulcus pattern *subtypes*. These distinctions within each pattern type offer more fine-grained characterization of OFC structure. Given the prevalence of Type I in most of the general population, more fine-grained assessment of inter-individual variability (such as using pattern subtypes) may be necessary to derive substantial meaning in genetic underpinnings as future research examines increasingly larger sample sizes.

2. Materials and methods

2.1. Participants

Structural images were obtained from the Human Connectome Project (HCP). This public data set includes high-resolution MRI structural neuroimaging on 1200 participants. We restricted our sample and analysis to only include twin pairs among this data set (476 individuals). All twins in this cohort did not have any psychiatric or genetic diagnoses. Participants were excluded from the original study if they had significant psychiatric, neurological, or cardiovascular disease, history of substance abuse, and/or hospitalization. The full list of inclusion/exclusion criteria can be accessed in Supplemental Table 1 from a previously published paper describing this cohort (Van Essen et al., 2013). All pairs of twins were also the same sex, ages 22−36 years old, with a mean age of 29 years. The cohort consisted of 86 dizygotic twin pairs (53 female, 33 male) and 152 MZ pairs (92 female, 60 male). We extracted zygosity, sex, ethnicity, race, age, height, and BMI from the available study data and summarize these in Table 1.

2.2. Image acquisition, preprocessing, and sulcal pattern pipeline

Data were obtained from the Human Connectome Project (HCP) S1200 release (Van Essen et al., 2012) using outputs from both the *PreFreeSurfer* and *FreeSurfer* Pipelines described in Glasser et al. (2013). Participants were all scanned at Washington University, St. Louis, using a customized 3T 'Connectome Skyra' scanner (details described

Table 1
Population characteristics.

Demographics	MZ twins	DZ twins
Pairs/Subjects (% of total)	152/304 (63.9%)	86/172 (36.1%)
Mean Age (SD)	29.4 (3.3)	29.1 (3.6)
Mean Height in Inches (SD)	67.0 (3.7)	67.7 (3.7)
Mean BMI (SD)	26.3 (4.7)	26.3 (5.4)
Male:Female Pairs (% of total)	60:92 (25.2%:38.7%)	33:53 (13.9%:22.3%)
Race and Ethnicity*	**MZ twin pairs**	**DZ twin pairs**
Asian/Nat. Hawaiian/Other Pacific Is.	5 (3.3%)	4 (4.7%)
Black/African Am. Non-Hispanic/ Latinx	14 (9.2%)	11 (12.8%)
White Non-Hispanic/Latinx	124 (81.6%)	65 (75.6%)
Unknown/Unreported	4 (2.6%)	5 (5.8%)

*Percentages for race and ethnicity are out of each twin cohort. Classifications that represented 2% or less of each cohort were excluded from the table, but included: Multiracial Hispanic/Latinx (0.7% MZ), Multiracial Non-Hispanic/ Latinx (0.7% MZ, 1.2% DZ), White Hispanic/Latinx (2.0% MZ).

elsewhere) (Gao et al., 2021). From the *PreFreeSurfer* pipeline, we utilized the T1 weighted MPRAGE (TR 2400 ms, TE 2.14 ms, flip angle = 8°, FOV 224 × 224 mm^2, voxel size = 0.7 mm isotropic, scan time = 7:40 min) that were aligned to standard MNI space. From the *FreeSurfer* pipeline, we retrieved an image of the cortical gray matter ribbon, which was converted into NIFTI format.

OFC sulcal extraction was performed using BrainVISA, for which we have validated OFC sulcal characterization in previous work (Snyder et al., 2019). The BrainVISA software can import FreeSurfer inputs converted into NIFTI volumetric format to help delineate tissue boundaries when reconstructing the cortical surface (Rivière et al., 2003). This reconstructed mesh of the cortical surface determines traces of sulci that fill the spaces between gyri along the cortical mantle. Following the pipeline described in Snyder et al. (Snyder et al., 2019), we extracted binary images of the OFC sulcal group. Interestingly, some subjects' sulci were consistently mislabeled upon several attempts at reprocessing. To still retain their OFC sulcal tracings, we automatically extracted all elementary cortical folds output by BrainVISA that fell within a mask of the OFC based on a previous study (Patti and Troiani, 2018). The term 'elementary cortical folds' is used within BrainVISA to describe the representation of contiguous sets of voxels without junctions, and thus this procedure leniently includes extra voxels in the tracing. These lenient tracings were only used for subjective characterizations of OFC sulcal patterns, for which these extra voxels can be readily ignored.

2.3. Categorical analysis of sulcal patterns

Following from our previous work (Patti and Troiani, 2018; Patti et al., 2020; Snyder et al., 2019), overarching OFC sulcogyral pattern types based on the continuity or discontinuity of the medial orbital sulcus (MOS) and lateral orbital sulcus (LOS) were determined. Pattern type is characterized for each hemisphere of the brain with Type I having a continuous LOS and discontinuous MOS, Type II having both a continuous MOS and LOS, Type III having both a discontinuous MOS and LOS, and Type IV having a continuous MOS and discontinuous LOS. Raters were unaware of the zygosity status of the subject or the relationship between subjects. Raters individually characterized pattern types using our established procedures. For any disagreement in the initial characterizations, the two raters reviewed the subject together and consensus was reached. This consensus procedure can be particularly useful as we have found that true disagreement is rare; rather, disagreement tends to stem from misidentification of a sulcus and/or failure to apply appropriate rules for individual sulcus determination. The consensus pattern was used for all subsequent analyses. To calculate inter-rater reliability consistent with other published work that only uses 1 primary rater, we randomly selected 20 hemispheres and a third rater (V.T.) characterized overall patterns. This inter-rater reliability was high (kappa: 0.85). See Fig. 1 for examples of individual pattern types.

2.4. Twin concordance

After pattern types were categorized, the resulting types (I, II, III, or IV) for each hemisphere of an individual were compared to those of their twin to determine concordance. Each pair was assigned a binarized score for both the left and right hemispheres indicating whether the overall pattern type was shared by both twins. For example, if Twin A's left hemisphere was categorized as Type I and Twin B's left hemisphere was also Type I, a score of "1" would indicate pattern concordance for the hemisphere. If Twin A's left hemisphere was Type I and Twin B's was Type III, a score of "0" would indicate the patterns were not in concordance. The percent of each population (MZ and DZ, left and right hemispheres) that shared sulcogyral pattern types was calculated based on typing classification (I-IV). As previous work has noted Type I to be the most common pattern, present in over half of the population (15), we also completed analyses separately for Type I patterns vs. a combination of all the other pattern types (II, III, and IV), based on the premise that Types II, III, and IV are less common and have been associated with schizophrenia and other psychiatric illness (Chakirova et al., 2010; Isomura et al., 2017; Lavoie et al., 2014; Nakamura et al., 2007; Takayanagi et al., 2010; Patti and Troiani, 2018).

2.5. Pattern subtype characterization

Although most of the previous work has focused only on the overall pattern types I-IV in the OFC, there is variance in the spatial relationship between OFC sulci that is not captured within the overall OFC pattern type, which we refer to as pattern *subtypes*. In Chiavaras and Petrides seminal work (Chiavaras and Petrides, 2000), they described this variation using cartoon drawings, with 6 different variations of Type I, 6 of Type II, and 6 of Type III (the Type IV pattern was not observed in the seminal paper). As an example of the features that influence subtype variability, individuals with a Type II pattern type may have different orientations of the MOS through the axial plane. See Fig. 2 for cartoon examples of a selection of pattern subtypes. There is also variability seen in the continuity of the MOS and LOS with the transverse orbital sulcus (TOS), the lengths of the individual sulci, and other identifying features. We have recently published additional pattern subtypes based on our ongoing work in several patient groups (Patti et al., 2020) and have demonstrated additional variability that was not present in the seminal population. For additional reference on features that are used to differentiate subtypes in this process and a complete visual depiction of pattern subtypes and subtype frequencies, please see **Supplementary Table S1 and Supplementary Figs. S1 and S2**.

Following overall pattern typing procedures described above, the OFC sulcal groups were then reviewed by two researchers that identified the pattern subtype. Both raters were unaware of the zygosity status of the subject or the relationship between subjects. Subtyping was completed by first uploading an individual OFC sulcal group file into BrainVISA's Anatomist image viewer (Rivière et al., 2003), manually labeling the individual rostral and caudal sulci of the MOS, TOS, LOS, and IOS. This step is important, as the automated process only identifies the overall OFC sulcal group, but not individual OFC sulci. Since BrainVISA-defined elementary folds within the OFC do not always segment along OFC sulcal boundaries defined in traditional OFC pattern typing, occasionally Anatomists' "split fold control" tool was used to split an elementary fold along such a boundary. Segmentations of OFC sulci were then converted into voxel-wise maps of the MOS and LOS in each hemisphere.

The labeled Anatomist image was then viewed in ITK-SNAP (Yushkevich et al., 2006) to display a color-coded, three-dimensional image of

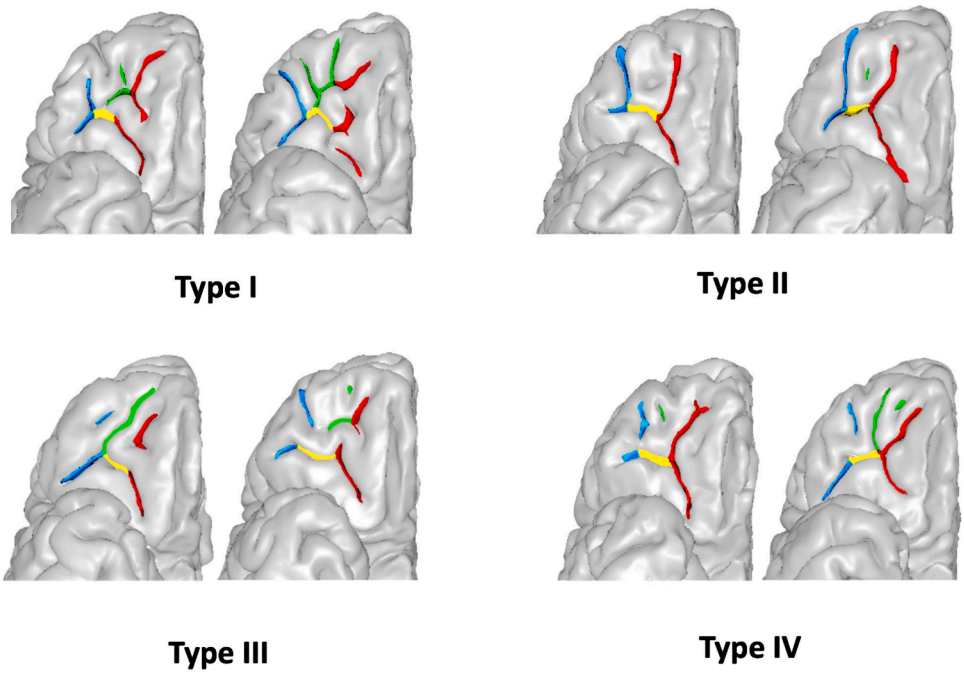

Fig. 1. Four orbitofrontal cortex pattern types. Four examples each of Type I, II, III, and IV patterns, with individual orbitofrontal sulci labeled. Medial orbital sulcus (MOS) is labeled in red, lateral orbital sulcus (LOS) in blue, intermediate orbital sulcus (IOS) in green, and transverse orbital sulcus (TOS) in yellow. The Type I pattern has a discontinuous MOS and continuous LOS, the Type II a continuous MOS and continuous LOS, the Type III a discontinuous MOS and discontinuous LOS, and Type IV a continuous MOS and discontinuous LOS. Right hemisphere only is presented in the figure

the subject's OFC sulcogyral pattern. The subject's subtype was determined based on several characteristics, including continuity, arrangements, and lengths of the MOS, TOS, LOS, and IOS. Subtype determination was initially determined by one rater (SK) and reviewed by a second rater (MAP) until consensus was reached or a novel subtype was identified. A detailed flowchart with key characteristics distinguishing subtypes from one another was used as a reference during the subtype characterization process by both researchers. We have found that maintaining this type of reference helps to characterize subtypes within the existing framework as well as to keep a systematic approach to new subtype characterization. Both visual and written descriptions of each previously identified and newly characterized subtype was also used in the subtype identification process. (**See Supplementary Text and Figures**).

2.6. Principal components analysis

In addition to more standard characterization procedures and analyses described above, we also completed a principal components analysis (PCA) as a method of data reduction and to better understand the relationship between pattern subtypes. To complete the PCA analysis, we first identified the 32 characteristics that comprise pattern subtypes (See **Supplementary Table S1**). Next, each individual subtype was represented by a unique sequence of 32 binary variables that indicate which characteristic is endorsed (x=1) or not endorsed (x=0) for a given subtype. Thus, each subtype was then represented as a vector based on whether each of the 32 features was endorsed or not for a given subtype. These characteristics were then used to classify any given pattern as a unique pattern subtype, independent of the original OFC pattern type (i.e., Type I, Type II, etc.). We then used PCA as a data reduction strategy to identify those characteristics that explained the maximum variation of pattern subtypes. In determining the number of characteristics (factors) that should remain, we evaluated scree tests for factors with an Eigen value $\geq$ 1.0. Those factors were then used to derive new subtype classifications for each of the primary Pattern Types. PCA analyses were performed using R Studio version 4.0.3 (R Core Team 2020) and the prcomp function (Sigg and Buhmann, 2008).

2.7. Probability map and shape manifold learning

Traditional, subjective descriptions of sulcogyral patterns group the patterns into two or more categories. To further highlight OFC variability in a continuous manner using a precedented data-driven approach, we adapted manifold learning methods from previously published work to our dataset. In brief, Sun et al. (Sun et al., 2012) represented each sulcus as a vector of the root mean square error distance to each other sulcus after pairwise coregistration of the sulcal maps. Left hemisphere sulci were flipped to match right hemisphere orientation. The Isomap algorithm, a type of manifold learning, is then used to map the matrix to a single dimension, for which moving averages of sulci along this dimension can depict the primary variation of sulcal shape. We deviate from the methods in Sun et al. only in how we visualize this dimension, since the methods were not built for sulci with prominent patterns of discontinuity. Therefore, we choose equidistantly spaced points along the full range of the dimension and averaged the 20 nearest sulcal shapes to each of these points. Following the gaussian blur procedure in Sun et al., we then threshold the images at a set value that permits only one discontinuity (two connected components) if prominent rostral and caudal segments constitute these two components.

The resulting shape index was computed separately for the MOS and LOS. Due to the manually intensive procedure of accurately delineating MOS and LOS boundaries at the voxel-level such that manifold learning can be sensitive to subtle shape variations, we retained a smaller dataset of 87 subjects (174 hemispheres) for this presentation of variability. The number of subjects included in this subset is consistent with previous work, which used a subset of 75 individuals (Sun et al., 2012).

Additionally, a heat map of OFC sulcal probability density was computed. Binary images of the full OFC sulcal group labeled by BrainVISA were simply averaged across all subjects to achieve this image. Positive values of sulcal probability in regions known to be outside the OFC were manually removed for visualization purposes. While previous work has created similar OFC sulcal probability maps (Perrot et al., 2011), the work here reflects OFC sulcal variability in this manner using the largest data set, to date.

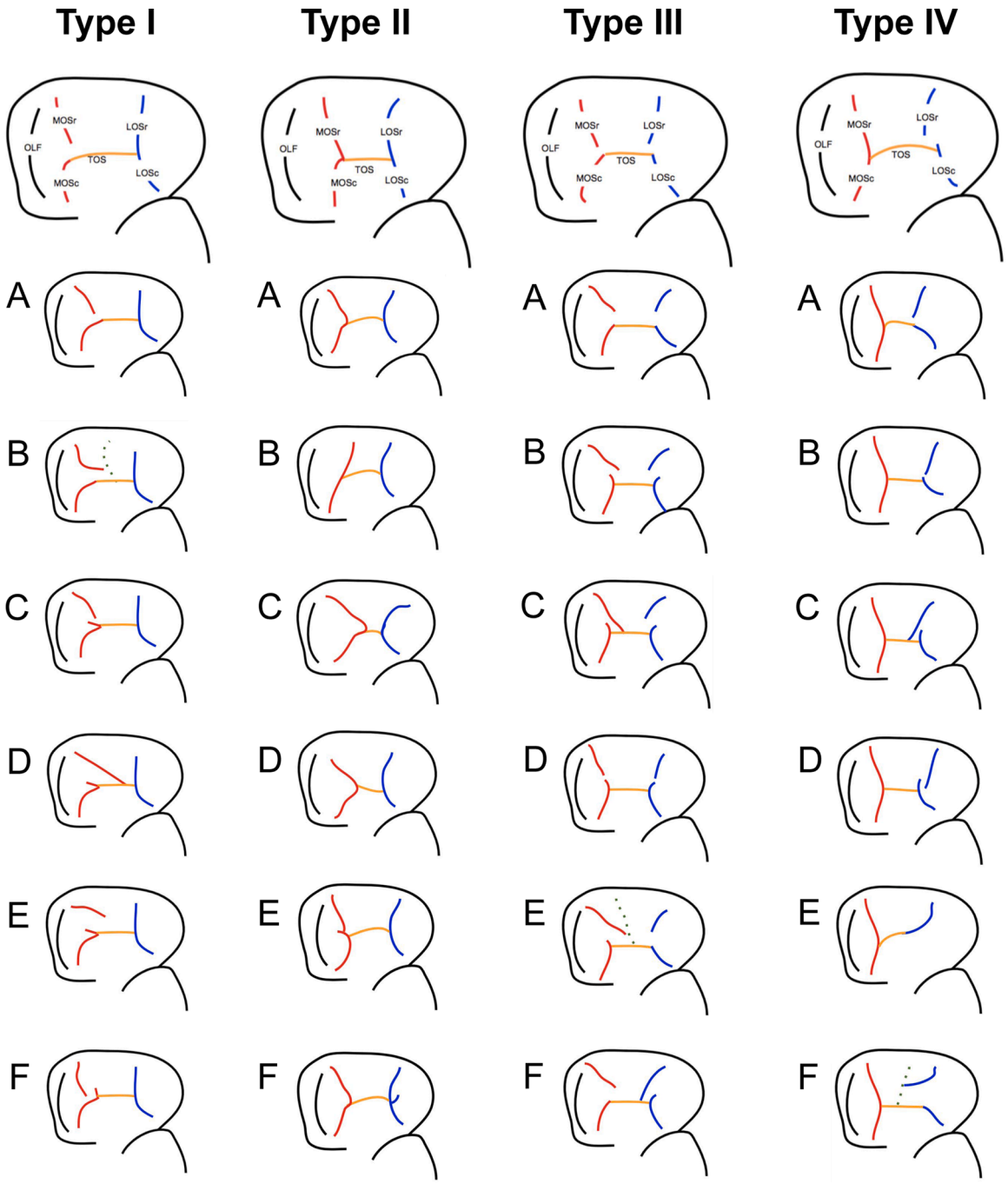

Fig. 2. Pattern subtypes. Cartoon depictions of first 6 examples of Type I, II, III, and IV pattern subtypes, named using a convention that follows from Chiavaras & Petrides (2000). Medial orbital sulcus (MOS) is labeled in red, lateral orbital sulcus (LOS) in blue, intermediate orbital sulcus (IOS) in green dotted, and transverse orbital sulcus (TOS) in yellow. Complete cartoon depictions and written description of differences between subtypes in Supplemental Figures and text.

3. Results

3.1. Overall pattern types/concordance for MZ and DZ overall patterns

We find that the frequency of pattern types within MZ and DZ twins are consistent with those in the general population [Type I, II, III, IV; MZ: 52%, 24%, 19%, 5%; DZ: 53%, 24%, 17%, 6%]. See Table 2. Bilateral concordance rates across all pattern types in DZ twins were 14% and 21% for MZ twins. We also calculated unilateral concordance for the most common pattern (Type I) vs. the less common patterns (Types II-IV). Type I patterns were 37% concordant for DZ and 35% concordant for MZ twins (right hemisphere) and 19% for DZ and 25% for MZ twins (left hemisphere). For Types II-IV, unilateral concordance on the right was 7% for DZ twins and 13% for MZ twins (right hemisphere) and 12% for DZ twins and 15% for MZ twins (left hemisphere). Overall, these results suggest minimal genetic influence on OFC pattern types. See Table 3.

Although inter-individual hemispheric concordance is not something that is frequently reported in the OFC sulcogyral analyses, we also summarize the prevalence of Type I bilateral concordance, Type II bilateral concordance, and so on, in Supplementary Table S3 We find that inter-individual bilateral concordance follows similar patterns to general pattern frequency, with Type I bilaterally being the most common, followed by Type II, III, and IV. Our current sample size is still

Table 2
Hemispheric typing frequency.[a]

	MZ	DZ
Overall Frequency	*N*=608	*N*=344
Type 1	52%	53%
Type 2	24%	24%
Type 3	19%	17%
Type 4	5%	6%
Right Hemisphere Frequency	*N*=304	*N*=172
Type 1	57%	60%
Type 2	21%	20%
Type 3	18%	17%
Type 4	3%	3%
Left Hemisphere Frequency	*N*=304	*N*=172
Type 1	48%	46%
Type 2	27%	28%
Type 3	19%	17%
Type 4	6%	8%

[a] N values represent the total number of hemispheres in each cohort (304 MZ individuals have 608 hemispheres; 86 DZ individuals have 172 hemispheres)

underpowered to examine intraindividual pattern typing within twin pairs, but we summarize the intra-individual pattern type twin concordance in **Supplementary Table S4**.

3.2. Overall description of subtypes found

We identified pattern subtypes that exist beyond those first described by Chiavaras and Petrides (Chiavaras and Petrides, 2000). In the seminal paper, 6 subtypes of each of the Type I, II, and III patterns were identified (18 total subtypes; labeled A-H; *N*=100 hemispheres). In the current work, we identified 87 total subtypes across Type I, II, III, and IV (*N*=458 hemispheres). This included 22 subtypes for Type I (A-V), 12 subtypes for Type II (A-L), 41 subtypes for Type III (A-AO), and 12 subtypes for Type IV (A-L) (**See Supplemental Fig. S1A–D**). We also quantified frequencies for each unique subtype to report distribution of subtype variability within each pattern type (**Supplemental Fig. S2A–D**).

It is unsurprising that Type III had the most variability in subtypes, as this pattern's distinguishing features include a discontinuous MOS *and* a discontinuous LOS. There is generally more variability in the potential for subtype features if a sulcus is discontinuous and thus, Type III patterns represent the overall pattern with the greatest potential for subtypes. Although we identified a large number of subtypes, it is important to mention that many individuals could be characterized with just a few subtypes. That is, approximately 62% of subjects with a Type I pattern had either subtype A or B, 55% of subtypes in subjects with Type II had subtypes A or D, 25% of Type III patterns were subtype A, and 33% of Type IV subtypes were A.

4. PCA results

The PCA analysis yielded 12 factors, explaining 78.94% of the total variation in pattern subtype characteristics. Using these 12 characteristics exclusively, we defined all unique pattern subtypes based on the sequence of response variables for these 12 items. This allowed for the PCA derived groupings of pattern subtypes, based on those characteristics that were identified as most important in explaining variability. Most of these characteristics were specific to describing the orientation of the LOS, and the intersections of the MOS and LOS with the TOS.

Using the results from the PCA analysis, we successfully reduced the number of pattern subtypes from *n*=22 subtypes for Type I to *n*=15, *n*=12 subtypes for Type II to *n*=7, *n*=41 subtypes for Type III to n=29, n=12 subtypes for Type IV to *n*=9. Results of the PCA analysis are available in Table 4. Frequencies of PCA derived subtypes by pattern types are displayed on radial plots in Fig. 3.

Table 3
Concordance.

Right Hemisphere

Overall		Twin B 1	2	3	4
Twin A	1	36%	11%	11%	1%
	2	12%	6%	4%	1%
	3	8%	1%	5%	2%
	4	2%	1%	0.4%	0%

MZ Twins		Twin B 1	2	3	4
Twin A	1	35%	10%	10%	1%
	2	14%	7%	3%	1%
	3	8%	1%	6%	3%
	4	1%	0%	0%	0%

DZ Twins		Twin B 1	2	3	4
Twin A	1	37%	12%	13%	0%
	2	9%	5%	5%	1%
	3	9%	1%	2%	0%
	4	2%	2%	1%	0%

Left Hemisphere

Overall		Twin B 1	2	3	4
Twin A	1	23%	12%	8%	2%
	2	14%	9%	3%	3%
	3	10%	4%	4%	1%
	4	3%	2%	1%	1%

MZ Twins		Twin B 1	2	3	4
Twin A	1	25%	9%	8%	2%
	2	16%	9%	4%	4%
	3	10%	5%	5%	1%
	4	2%	1%	0%	1%

DZ Twins		Twin B 1	2	3	4
Twin A	1	19%	17%	9%	1%
	2	10%	9%	2%	1%
	3	10%	3%	2%	1%
	4	6%	3%	3%	0%

Frequencies of PCA derived pattern subtypes were relatively similar for the right and left hemispheres, particularly for pattern Type I and Type II. We observed slightly more variation in PCA derived pattern subtypes between the hemispheres for pattern Type III and Type IV.

5. Probability map and shape manifold learning results

We additionally resolved the variability of OFC sulcal morphology with two data-driven approaches. Both approaches appear to align with pattern-based, categorical analyses, reinforcing that such pattern typing captures the meaningful variation in OFC sulcal morphology. First, the spatial probability density map of OFC sulci largely resembles the most frequently occurring Type I pattern, whose disproportionate representation in the population drives its resemblance in the heat map (Fig. 4a). Additionally, the MOS and LOS shape indices based on manifold learning methods align with categorical definitions of OFC variability. Even along a continuous axis, the primary variability appears to be with the continuity of the MOS and LOS. Shifts in sulcal continuity along this dimension also appear to coincide with shifts in the orientation of rostral and caudal segments (Fig. 4b). The orientations of broken sulci along the shape index are consistent with the orientation of branching sulcal segments in OFC subtypes that include a discontinuous MOS or LOS.

Table 4
Items[a] used to differentiate subtypes within pattern types, ranked by proportion and percentage of variance explained from principal component analyses.

Question[b]	Percentage Variance Explained
Q20. Is the LOSr continuous with the LOSc?	15.91
Q2. Is the MOSr continuous with the MOSc?	11.21
Q28. Is the LOSr oriented on the same path as the LOSc?	8.637
Q32. Does the LOS form a straight line?	7.357
Q19. Is the LOSr independent from all other sulci?	7.099
Q11. Is the MOSr oriented on the same path as the MOSc?	5.242
Q26. Does the LOSc extend past the TOS?	4.701
Q21. Does the LOSr intersect with the TOS?	4.244
Q3. Does the MOSr intersect with the TOS?	4.095
Q7. Does the MOSc end at the TOS?	3.826
Q15. Does the MOS form a straight line?	3.387
Q12. Does the MOSr extend towards the lateral side of the MOSc?	3.23
Q4. Does the MOSr intersect with the IOS?	3.131
Q27. Is the LOSc absent?	2.728
Q8. Does the MOSc extend past the TOS?	2.483
Q31. Does the LOS have multiple branches?	2.478
Q14. Does the MOS have multiple branches?	2.041
Q24. Does the LOSc intersect with the TOS?	1.624
Q30. Does the LOSr extend toward the medial side of the LOSc?	1.599
Q23. Is the LOSc independent from all other sulci?	1.429
Q1. Is the MOSr independent from all other sulci?	0.849
Q13. Does the MOSr extend towards the medial side of the MOSc?	0.651
Q16. Is the MOS oriented diagonally?	0.58
Q25. Does the LOSc end at the TOS?	0.375
Q17. Is the TOS present?	0.268
Q6. Does the MOSc intersect with the TOS?	0.248
Q29. Does the LOSr extend toward the lateral side of the LOSc?	0.214
Q9. Is the MOSc absent?	0.16
Q22. Does the LOSr Intersect with the IOS?	0.085
Q5. Is the MOSc independent from all other sulci?	0.073
Q10. Is the MOSr is oriented horizontally?	0.04
Q18. Is the TOS continuous with itself?	0

MOS: Medial Orbital Sulcus, MOSr: Rostral MOS, MOSc: Causal MOS, LOS: Lateral Orbital Sulcus, LOSr: Rostral LOS, LOSc: Caudal LOS, TOS: Transverse Orbital Sulcus, IOS: Intermediate Orbital Sulcus,
NOTE: The original ordering of each unique question does not have any bearing on the importance of this question in determining overall pattern subtype

[a] Questions are not inherently specific to pattern types, however there are some items that are only specific to some pattern types (i.e., "Does the MOSr intersect with and IOS?" can only be endorsed in cased where the MOS is discontinuous, and thus cannot be considered for pattern type II).

[b] Each item corresponds to a yes or no response.

6. Discussion

The results from this study indicate that both MZ and DZ twins of the same sex have a distribution of OFC sulcogyral patterns that are consistent with previous work in singletons. This indicates that there is nothing inherent in a multiple gestation environment that changes pattern type frequency from what is expected from previous work in adults that lack psychiatric diagnoses. We also find that there is only a small difference in concordance rates between MZ and DZ twin pairs, which suggests there is minimal genetic influence on OFC pattern types. In addition to being the first study to characterize OFC sulcogyral patterns in twins, this work also represents the largest population of individuals with OFC pattern type characterizations, to date, which can then serve as an important resource towards understanding the variability of these patterns overall in the population.

Previous work exploring brain similarities in twin studies have mixed findings regarding heritability of brain volume and/or surface morphology measurements. Several studies reported minimal genetic influence on surface morphology (Bartley, 1997; Hasan et al., 2011) or sulcal presence (Amiez et al., 2018), while volumetric features, such as grey matter volume, were found to be more similar in MZ twins (White, 2002). However, other work has found that surface metrics such as convexity, curvature, and sulcal width are heritable near major sulci and primary fissures, whereas metrics of secondary sulci are largely non-heritable (Schmitt et al., 2021). When assessing whether measures of cortical thickness were heritable and influenced functional connectivity, recent work demonstrated that cortical thickness has a genetic basis and is related to local connectivity (Alexander-Bloch et al., 2013). However, this correspondence between neuroanatomical curvature and local connectivity was less pronounced in the prefrontal cortex and other regions of association cortex (Alexander-Bloch et al., 2020). There is also evidence that category-selective regions of the brain (defined based on functional responsivity within anatomical boundaries) are more similar in MZ than DZ twins and that voxels with responsivity linked more to genetic similarity tend to be located on regions of curvature (gyral crowns or sulcal fundi) (Abbasi et al., 2020). Thus, while there is not a consensus as to the most heritable surface topology metrics, some features (convexity, curvature, sulcal width, cortical thickness) appear to be heritable near major sulci and primary fissures.

None of the previously described surface morphology metrics include sulcal discontinuity, which is the primary feature that differentiates orbitofrontal cortex H-sulcal pattern types. Further, one of the primary differences between previous examinations of twin brain morphology and ours is that we use a more qualitative pattern type characterization method, rather than a fully automated extraction of sulcal metrics. Although we ultimately draw similar conclusions that sulcal variability in the OFC is likely influenced by environmental factors, the key difference between OFC pattern characterization procedures described here and other sulcal metrics (like gyrification indices) is that meaningful variability can be resolved with high fidelity at the individual/patient level. Given the ability to interpret OFC pattern type at the patient level along with previous findings that certain pattern types may contribute to risk for schizophrenia and other psychiatric disorders (Chakirova et al., 2010; Isomura et al., 2017; Lavoie et al., 2014; Nakamura et al., 2007; Takayanagi et al., 2010; Patti and Troiani, 2018), developing a deeper understanding of OFC pattern types is warranted and may contribute to precision medicine approaches (Hodson, 2016), such as assessment of heightened risk for psychiatric illness. From that perspective, future work assessing the utility of sulcogyral pattern typing alongside other risk factors (such as rare genetic changes) may indicate whether more qualitative morphological markers inform

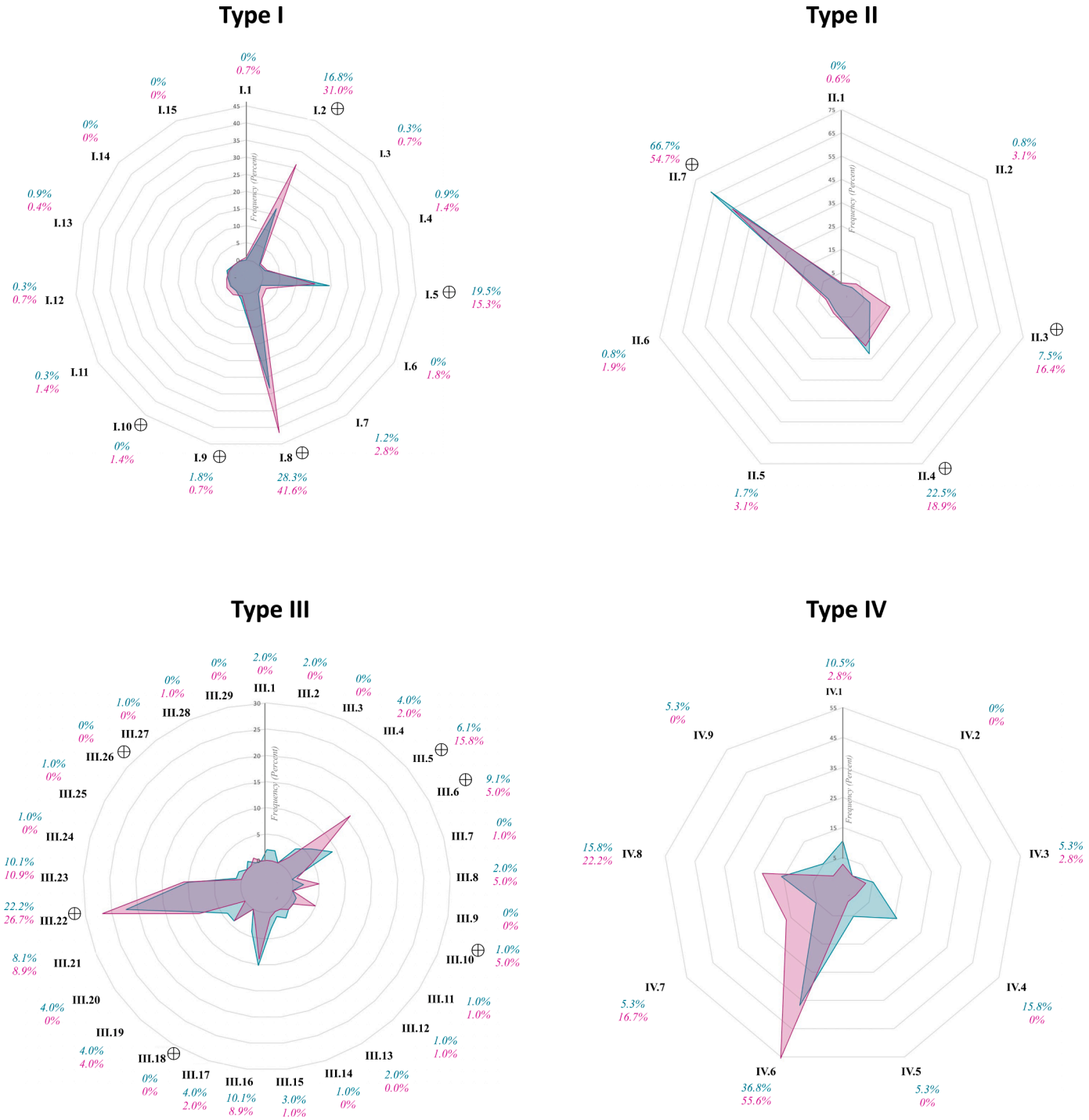

Fig. 3. Radar plots of derived subtypes from Principal Components Analysis of OFC Pattern Types for left and right hemispheres. Derived subtypes along axis follow the naming convention (OverallPatternType.DerivedPatternNumber; I.1). Subtypes marked with an ⊕ include at least one of the original 6 subtypes from Chiavaras & Petrides (2000). Right hemisphere values plotted in teal and left hemisphere plotted in pink, with corresponding percentages of the population with each subtype for each hemisphere depicted in corresponding colors along the outer axis of the plot for each derived subtype.

overall psychiatric disease risk. Future work may also benefit from conducting similar twin studies in samples with psychiatric illness. Comparing our findings within a sample that lacks psychiatric diagnoses to those with known psychopathology can provide insights towards uncovering the influence of genetics and environment on psychiatric illness development.

In addition to our main goal of characterizing whether pattern type prevalence differs between MZ and DZ twins, we also describe and operationalize a process to document pattern subtypes. The concept of subtypes and this documentation procedure was first completed by Chiavaras and Petrides (2000) in their seminal work, but continued pattern subtyping has not been documented in the many papers that have established OFC sulcogyral pattern frequency in the general population. Subtyping may be important for future studies to adapt to better understand the full range of pattern subtypes, as well as to continue data-driven strategies to derive new pattern subtypes or to reveal previously undescribed relationships between pattern types and/or subtypes.

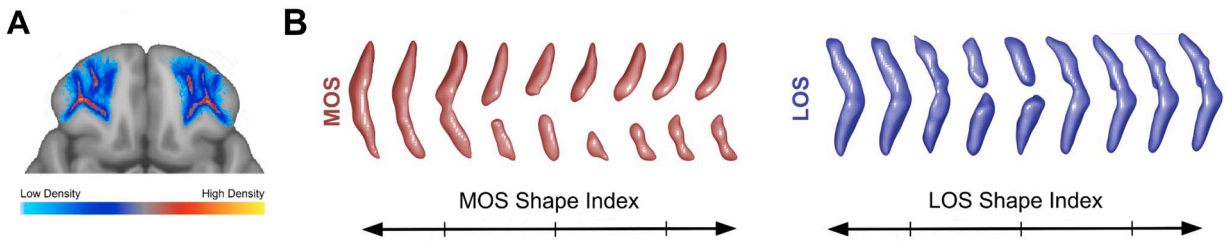

Fig. 4. OFC Sulcogyral Variability. (A) Probability density plot generated by averaging binary images of all subject's OFC sulcal groups. Regions of high density indicate high density of overlap across subjects and thus high probability of any given subject having an OFC sulcus located at that region.(B) Isomap primary axes of variation for Medial Orbital Sulcus (MOS) and Lateral Orbital Sulcus (LOS). To visualize the organization of the Isomap, all sulci are first aligned to the template sulcus using the optimal transformation generated by the algorithm. The template that is used for alignment reflects the sulcus that minimizes the average distance between the given sulcus and the rest of the set. Each sulcus is then translated along the anterior-posterior axis to its appropriate Isomap coordinates.

It is expected that as the field continues to assess OFC patterns in larger and more diverse populations, observed variance in patterns will likely expand. Case in point, the seminal study only described 3 pattern types. The 4th overall type, characterized by a continuous MOS and discontinuous LOS was not observed in the seminal sample of 50 human brains, but added in subsequent work as study samples diversified. The current sample of 476 people is increased by nearly 10-fold from the seminal sample, while the number of observed variations (subtypes) only increased by less than 5-fold. The results of our principal components analysis indicate that a handful of subtypes (including many of the original subtypes) can be used to describe most of the sample. This indicates that there is some meaning in the original patterns and subtypes that continue to be represented in more diverse populations with highest frequency. Importantly, we have operationalized a process here for data reduction that may lend itself to our future understanding of OFC pattern types that are driven by multiple features, rather than just MOS and LOS continuity.

It is important to consider our findings in the context of the original findings of Chiavaras and Petrides (2000), which found similar H-sulcus patterns appearing in the OFC of macaques. Evidence of shared homology across species is typically thought to indicate a preserved relationship between a given region of cortex and the function of its underlying architecture in behavior, possibly with similar genetic origins. Understanding whether there is conservation of specific features across species is thought to be helpful in determining whether these features serve a common basic function or developmental role. In addition, understanding whether different species have a homologous region to their human counterparts allows for a deeper understanding of the brain and allows for translational research from non-human model systems. Some evolutionary perspectives have suggested that folding patterns may be driven more by brain volume and corresponding mechanical constraints on the folding process, rather than phylogeny (Heuer et al., 2019). This perspective aligns with there being similar but not genetically distinguished patterns of OFC folding in the human brain, and indicates we have additional work to do to fully understand how volumetric differences may drive some morphological markers and interact with genetic mediators. Related to this point, a study of MZ twin pairs used differences in birth weight as a proxy for differences in the utero environment and found that discordance was positively associated with both cortical surface area and cortical volume discordance (Raznahan et al., 2012). The authors concluded that differences in methylation that occur based on the *in utero* environment mediate cortical surface morphology.

Here, we focus on one marker of sulcogyral variability in the H-sulcus, but there is a growing body of work examining other more qualitative, second order patterns that are formed by the intersection of multiple sulci. Examples of these include the anterior cingulate (CIT), the power button symbol (Mellerio et al., 2015), and the omega in fusiform cortex (Weiner et al., 2014, Weiner and Zilles, 2016). In addition, other sulcogyral landmarks, such as "plis de passage" or annectant gyri, have been proposed as potential landmarks for studying individual differences in the brain (Mangin et al., 2019, Bodin et al., 2021). We and others have been working towards automated and semi-automated pipelines to objectively identify known higher-order shapes and characterization of such landmarks in the brain (Snyder et al., 2019, Borne et al., 2021). Although brain-gene relationships at the genome-wide level are still in their infancy (Zhao et al., 2019, Elliott et al., 2018), future work may benefit from incorporating second order sulcogyral metrics such as those described here.

There are several limitations to the current study. We used existing data that was collected as part of a large-scale effort known as the Human Connectome Project (HCP). This effort includes screening measures that exclude individuals with known psychiatric illness and thus, the data available for this study did not include twins with psychiatric diagnoses. Future work should examine OFC morphology in twin pairs where one twin is diagnosed with a disorder known to disrupt OFC patterns. Another limitation of the current data set is that to be included in the study, all twin pairs were required to reach full term (i.e. 34 weeks gestation for twins). We did not have information on precise gestational age and/or birth weight for this cohort, which have been found to be related to differences in cortical thickness between twins (Casey et al., 2017). It would be beneficial for future work to include comprehensive information on metrics captured at time of birth in twins, rather than only information related to enrollment surrounding adulthood. As we did not observe evidence to suggest strong genetic heritability of OFC pattern type among twin pairs, future work may also consider the impact of gestational or early life environmental exposures on OFC pattern type. We did not examine the influence of sex on sulcogyral patterns, as previous work has not found any influence of sex on sulcogyral pattern frequency. We are not powered in the current sample to examine inter-individual concordance on pattern subtypes. However, we have included tables that illustrate inter-individual concordance in subtypes in Supplementary Table 3. Finally, FreeSurfer outputs are prone to poor registration of sulcal landmarks in tertiary folds (Auzias et al., 2013), thus it may be important for future work to explore methodological advances that allow for alignment in more variable, tertiary folds- and allow for calculation of concordance metrics within OFC sulci that are not solely qualitative. While the lack of concordance in the overall pattern types may at face value seem to call into question the utility of pattern subtypes overall, we argue that this intermediate methodological step that may prove to be useful as we continue to increase sample size.

Overall, the results presented here demonstrate that OFC sulcogyral morphology, as measured using H-sulcus pattern typing, shows similar frequencies in both MZ and DZ twin pairs. This work represents the first characterization of twin pairs using this procedure, as well as the largest (N=476) characterization of OFC pattern types in any population, to date. Taken together with other studies in twin pairs, the minimal influence of genetics in the sulcogyral morphology of the OFC and other regions of cortex that develop later in fetal gestation may capture

important variance that is not genetic in origin but is relevant to psychiatric disease risk.

Declaration of Competing Interest

The authors have no conflicts of interest.

Supplementary materials

Supplementary material associated with this article can be found, in the online version, at doi:10.1016/j.pscychresns.2022.111492.

References

Abbasi, N., Duncan, J., Rajimehr, R., 2020. Genetic influence is linked to cortical morphology in category-selective areas of visual cortex. Nat. Commun. 11, 709.

Alexander-Bloch, A., Giedd, J.N., Bullmore, E., 2013. Imaging structural co-variance between human brain regions. Nat. Rev. Neurosci. 14, 322–336.

Alexander-Bloch, A.F., et al., 2020. Imaging local genetic influences on cortical folding. Proc. Natl. Acad. Sci. U. S. A. 117, 7430–7436.

Amiez, C., Wilson, C.R.E., Procyk, E., 2018. Variations of cingulate sulcal organization and link with cognitive performance. Sci. Rep. 8, 13988.

Armstrong, E., Schleicher, A., Omran, H., Curtis, M., Zilles, K., 1995. The ontogeny of human gyrification. Cereb. Cortex 5, 56–63.

Auzias, G., et al., 2013. Model-driven harmonic parameterization of the cortical surface: HIP-HOP. IEEE Trans. Med. Imaging 32, 873–887.

Bartley, A., 1997. Genetic variability of human brain size and cortical gyral patterns. Brain 120, 257–269.

Bodin, C., et al., 2021. Plis de passage in the superior temporal sulcus: Morphology and local connectivity. NeuroImage 225, 117513.

Borne, L., et al., 2021. Automatic recognition of specific local cortical folding patterns. NeuroImage 238, 118208.

Cachia, A., et al., 2016. Longitudinal stability of the folding pattern of the anterior cingulate cortex during development. Dev. Cogn. Neurosci. 19, 122–127.

Cachia, A., et al., 2021. Towards deciphering the fetal foundation of normal cognition and cognitive symptoms from sulcation of the cortex. Front. Neuroanat. 15, 712862.

Casey, K.F., et al., 2017. Birth weight discordance, DNA methylation, and cortical morphology of adolescent monozygotic twins: birth weight, methylation, and brain morphology. Hum. Brain Mapp. 38, 2037–2050.

Chakirova, G., et al., 2010. Orbitofrontal morphology in people at high risk of developing schizophrenia. Eur. Psychiatr. 25, 366–372.

Chi, J.G., Dooling, E.C., Gilles, F.H, 1977. Gyral development of the human brain. Ann. Neurol. 1, 86–93.

Chiavaras, M.M., Petrides, M., 2000. Orbitofrontal sulci of the human and macaque monkey brain. J. Comp. Neurol. 422, 35–54.

Chye, Y., et al., 2017. Role of orbitofrontal sulcogyral pattern on lifetime cannabis use and depressive symptoms. Prog. Neuro Psychopharmacol. Biol. Psychiatry 79, 392–400.

Delahoy, R., et al., 2019. An examination of orbitofrontal sulcogyral morphology in obsessive–compulsive disorder. Psychiatry Res. Neuroimaging 286, 18–23.

Dubois, J., et al., 2008. Mapping the early cortical folding process in the preterm newborn brain. Cereb. Cortex 18, 1444–1454.

Dubois, J., et al., 2019. The dynamics of cortical folding waves and prematurity-related deviations revealed by spatial and spectral analysis of gyrification. NeuroImage 185, 934–946.

Elliott, L.T., et al., 2018. Genome-wide association studies of brain imaging phenotypes in UK Biobank. Nature 562, 210–216.

Gao, S., et al., 2021. Comparing empirical kinship derived heritability for imaging genetics traits in the UK biobank and human connectome project. NeuroImage 245, 118700.

Garcia, K.E., Kroenke, C.D., Bayly, P.V., 2018. Mechanics of cortical folding: stress, growth and stability. Philos. Trans. R. Soc. B 373, 20170321.

Glasser, M.F., et al., 2013. The minimal preprocessing pipelines for the Human Connectome Project. NeuroImage 80, 105–124.

Habas, P.A., et al., 2012. Early folding patterns and asymmetries of the normal human brain detected from in utero MRI. Cereb. Cortex 22, 13–25.

Hasan, A., et al., 2011. Prefrontal cortex gyrification index in twins: an MRI study. Eur. Arch. Psychiatry Clin. Neurosci. 261, 459–465.

Heuer, K., et al., 2019. Evolution of neocortical folding: a phylogenetic comparative analysis of MRI from 34 primate species. Cortex 118, 275–291.

Hodson, R., 2016. Precision medicine. Nature 537. S49–S49.

Im, K., et al., 2011. Quantitative comparison and analysis of sulcal patterns using sulcal graph matching: a twin study. NeuroImage 57, 1077–1086.

Isomura, S., et al., 2017. Altered sulcogyral patterns of orbitofrontal cortex in a large cohort of patients with schizophrenia. npj Schizophr. 3, 3.

Jiang, X., Zhang, T., Zhang, S., Kendrick, K.M., Liu, T., 2021. Fundamental functional differences between gyri and sulci: implications for brain function, cognition, and behavior. Psychoradiology 1, 23–41.

Lavoie, S., et al., 2014. Sulcogyral pattern and sulcal count of the orbitofrontal cortex in individuals at ultra high risk for psychosis. Schizophr. Res. 154, 93–99.

Lenroot, R.K., et al., 2009. Differences in genetic and environmental influences on the human cerebral cortex associated with development during childhood and adolescence. Hum. Brain Mapp. 30, 163–174.

Li, Y., et al., 2019. Altered orbitofrontal sulcogyral patterns in gambling disorder: a multicenter study. Transl. Psychiatry 9, 186.

Lyu, I., Kim, S.H., Girault, J.B., Gilmore, J.H., Styner, M.A., 2018. A cortical shape-adaptive approach to local gyrification index. Med. Image Anal. 48, 244–258.

Mangin, J.-F., et al., 2019. Plis de passage" deserve a role in models of the cortical folding process. Brain Topogr. 32, 1035–1048.

Mellerio, C., et al., 2015. The power button sign: a newly described central sulcal pattern on surface rendering MR images of type 2 focal cortical dysplasia. Radiology 274, 500–507.

Nakamura, M., et al., 2007. Altered orbitofrontal sulcogyral pattern in schizophrenia. Brain 130, 693–707.

Patti, M.A., et al., 2020. Orbitofrontal sulcogyral morphology in patients with cocaine use disorder. Psychiatry Res. Neuroimaging 305, 111174.

Patti, M.A., Troiani, V., 2018. Orbitofrontal sulcogyral morphology is a transdiagnostic indicator of brain dysfunction. NeuroImage Clin. 17, 910–917.

Peper, J.S., Brouwer, R.M., Boomsma, D.I., Kahn, R.S., Hulshoff Pol, H.E., 2007. Genetic influences on human brain structure: a review of brain imaging studies in twins. Hum. Brain Mapp. 28, 464–473.

Perrot, M., Rivière, D., Mangin, J.-F., 2011. Cortical sulci recognition and spatial normalization. Med. Image Anal. 15, 529–550.

R Core Team, 2020. R: A language and environment for statistical computing. R Foundation for Statistical Computing.

Rajagopalan, V., et al., 2011. Local tissue growth patterns underlying normal fetal human brain gyrification quantified in utero. J. Neurosci. 31, 2878–2887.

Raznahan, A., Greenstein, D., Lee, N.R., Clasen, L.S., Giedd, J.N, 2012. Prenatal growth in humans and postnatal brain maturation into late adolescence. Proc. Natl. Acad. Sci. U. S. A. 109, 11366–11371.

Rivière, D., Régis, J., Cointepas, Y., Papadopoulos-Orfanos, D., 2003. A freely available Anatomist/BrainVISA package for structural morphometry of the cortical sulci. NeuroImage 19, 934.

Schmitt, J.E., Raznahan, A., Liu, S., Neale, M.C., 2021. The heritability of cortical folding: evidence from the human connectome project. Cereb. Cortex 31, 702–715.

Sigg, C.D., Buhmann, J.M., 2008. Expectation-maximization for sparse and non-negative PCA. In: Proceedings of the 25th international conference on Machine learning - ICML '08. ACM Press, pp. 960–967. https://doi.org/10.1145/1390156.1390277.

Snyder, W., Patti, M., Troiani, V., 2019. An evaluation of automated tracing for orbitofrontal cortex sulcogyral pattern typing. J. Neurosci. Methods 326, 108386.

Sun, Z.Y., et al., 2012. The effect of handedness on the shape of the central sulcus. NeuroImage 60, 332–339.

Takayanagi, Y., et al., 2010. Volume reduction and altered sulco-gyral pattern of the orbitofrontal cortex in first-episode schizophrenia. Schizophr. Res. 121, 55–65.

Tissier, C., et al., 2018. Sulcal polymorphisms of the IFC and ACC contribute to inhibitory control variability in children and adults. eNeuro 5. ENEURO.0197-17.2018.

Van Essen, D.C., et al., 2013. The WU-Minn human connectome project: an overview. NeuroImage 80, 62–79.

Van Essen, D.C., et al., 2012. The human connectome project: a data acquisition perspective. NeuroImage 62, 2222–2231.

Vasung, L., et al., 2019. Exploring early human brain development with structural and physiological neuroimaging. NeuroImage 187, 226–254.

Weiner, K.S., et al., 2014. The mid-fusiform sulcus: a landmark identifying both cytoarchitectonic and functional divisions of human ventral temporal cortex. Neuroimage 84, 453–465.

Weiner, K.S., Zilles, K., 2016. The anatomical and functional specialization of the fusiform gyrus. Neuropsychologia 83, 48–62.

White, T., 2002. Brain volumes and surface morphology in monozygotic twins. Cereb. Cortex 12, 486–493.

Yoshimi, A., et al., 2016. Effects of *NRG1* genotypes on orbitofrontal sulcogyral patterns in Japanese patients diagnosed with schizophrenia: *NRG1* and schizophrenia. Psychiatry Clin. Neurosci. 70, 261–268.

Yushkevich, P.A., et al., 2006. User-guided 3D active contour segmentation of anatomical structures: significantly improved efficiency and reliability. NeuroImage 31, 1116–1128.

Zhao, B., et al., 2019. Large-scale GWAS reveals genetic architecture of brain white matter microstructure and genetic overlap with cognitive and mental health traits (n = 17,706). Mol. Psychiatry. https://doi.org/10.1038/s41380-019-0569-z.